A four-unknown higher-order shear deformation theory for the analysis of bending in sigmoid-FGM plates

Fatima Zohra Djidar[a], *Habib* Hebali[b]

[a.] Mustapha Stambouli University,Departement of Civil Engineering,Mascara,People's Democratic Republic of Algeria, e-mail: fatima.djidar@univ-mascara.dz. ORCID iD: https://orcid.org/0009-0006-6361-073X

[b.] Mustapha Stamnouli University, Departement of Civil Engineering,Mascara,People's Democratic Republic of Algeria,e-mail: habib.hebali@univ-mascara.dz ,**corresponding author**.ORCID iD: https://orcid.org/0009-0001-1309-2595

https://doi.org/10.5937/vojtehg73-57862

FIELD: civil engineering
ARTICLE TYPE: original scientific paper

Abstract:

In this paper, the analysis of bending of sigmoid functionally graded materials (S-FGM) plates is presented using a four-variable high-order shear deformation theory.This theory reduces the number of unknown functions simply from five to four compared to other shear deformation theories; it does not require shear correction factors, and it satisfies the conditions of zero shear stresses for the top and bottom surface of the plate since the variation of shear stresses is parabolic through the thickness. The equilibrium equations of this theory are derived from the principle of virtual work, and the Navier solution is used to solve these equations. For this S-FGM plate, according to the power law, the materials are distributed in terms of volume fractions of the constituents, and their properties are gradually varied in the thickness direction. This analytical study gave very satisfactory results, and the comparison between the numerical results obtained from the presented theory and those obtained from the classical plate theory (CPT) and high-order shear deformation theories (HSDTs) demonstrated the simplicity, accuracy, and reliability of this presented theory in analyzing the static bending behavior of thick S-FGM plates.
Methods:This study presents a four-variable shear deformation theory that determines the stresses and displacements of a simply supported functionally graded (S-FGM)plate. The equilibrium equations and boundary conditions were obtained from the principle of virtual work. Navier's method was then used to solve the equilibrium equations. The comparison of the results of this new theory with other solutions using the CPT and HSDTs was presented in this work.

Results:The comparison between the presented refined theory and the HSDT(Reddy's theory) also showed that the deformations and stresses of these theories are almost identical, while the classical plate theory underestimates the deflection of these plates.

Conclusion:The calculated different stresses and dimensionless displacements clearly demonstrated the effectiveness and accuracy of the presented theory in studying the static behaviors of simply supported S-FGM plates.

Key words:S-FGM plates, classical plate theory, higher-order theory, powerlaw, bending.

Introduction

In recent years, Functionally Graded Materials (FGMs) have seen wide applications in several diverse engineering and industrial fields such as civil, mechanical, electronic, automotive, aerospace, etc., due to their attractive and distinctive properties, which are high wear resistance, significant reduction in residual stresses and high resistance to temperature gradients (Reddy, 2000; Eltaher et al., 2013; Kar & Panda, 2015; Ahmed et al., 2019; Karami & Karami, 2019; Selmi, 2020; Abdulrazzaq et al., 2020; Dehshahri et al., 2020).

FGMs are used in these important fields in the form of plates, characterized by a gradual variation in the volume fraction of their constituent materials, which leads to a continuous and smooth change in the properties of these materials from one surface to another (Birman et al., 2013; Dai et al., 2016). This technology contributes to reducing thermal stress concentrations and effectively eliminating interface problems for devices using FGM plates, such as environmental sensors, biomedical industry, and fast computers (Avcar, 2015; Boukhari et al., 2016).

In order to effectively investigate the behavior of these FGM plates, many modern scientific studies have been conducted,leading to the development of different plates theories. Among these theories is the classical plate theory (CPT) which is considered the simplest theory because it does not take into account the effects of transverse shear of these plates. However, it gives very satisfactory analytical results withregard to isotropic and thin plates (Mechab et al., 2010; Taczała et al., 2022).

Since these transverse shear effects cause instability and failure of plates structures, especially composite plates, the First-order Shear Deformation Theory (FSDT), proposed by Mindlin (1951) and Reissner (1945), has been relied upon to conduct an effective study of FGM plates because they take these effects into account. However, it requires a

correction coefficient often set at 5/6 (Hosseini-Hashemi et al., 2010; Hosseini-Hashemi et al., 2011). The violation of equilibrium conditions at both the bottom and top surfaces of the FGM plate is considered the most significant drawback of the FSDT (Fallah et al., 2013), which necessitated the development of the Higher-order Shear Deformation Theory (HSDT). This theory takes into account the transverse shear effect and ensures the state of zero shear stresses in the top and bottom surfaces of the plate without the correction factor (Thai & Choi, 2012; Thai & Kim, 2013; Sobhy, 2013; Pandey et al., 2020).

Recently, plates based on Sigmoid Functionally Graded Materials (S-FGM plates) have been studied in a very precise analytical manner by (Beldjelili et al., 2016; Duc, 2017; Singh, Harsha, 2019; Singh, Harsha, 2020; Tao & Dai, 2021; Karakoti et al., 2022; Kurpa et al., 2023; Kumar & Pandey, 2024).

The aim of this work is to study the bending behavior of S-FGM plates using the present high-order theory with a sinusoidal shear function. The results obtained have been compared with those calculated using Reddy's shear function and the classical plate theory (CPT). To carry out an efficient and precise analytical study, the influence of the powerlaw index **p** on the deflection and different non-dimensional stresses of S-FGM plates made of aluminum/alumina mixture has been investigated for various values of the dimension ratios (a/h and a/b).

Refined FGM plate theory

Geometric configuration

Figure 1 presents a rectangular S-FGM plate with the dimensions a and b in the plane, as well as with a uniform thickness h. This S-FGM plate is made of a material with a property gradient that varies in the thickness direction, as shown in Figure 1, and is subjected to a transverse load q(x,y). TheCartesian coordinate system is used such that the x, y plane coincides with the median plane of the plate.

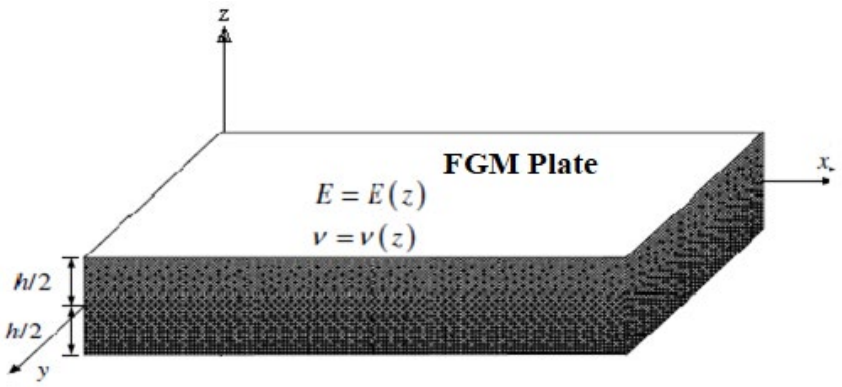

Figure 1 – Geometry of an FGM plate(Chi, Chung, 2006)

The S-FGM plate studied in this work is delimited by the planes at the coordinates x=0,a and y=0,b. The middle surface, defined by z=0, serves as the reference surface of this plate, where z represents the thickness coordinate measured from this undeformed middle surface. For an S-FGM plate with a ceramic-metal mixture, the functional relationship between E and z can be given as:

$$g_1(z) = 1 - \frac{1}{2}\left(\frac{h/2 - z}{h/2}\right)^p \text{ for } 0 \le z \le h/2$$

$$g_2(z) = \frac{1}{2}\left(\frac{h/2 + z}{h/2}\right)^p \text{ for } -h/2 \le z \le 0 \quad (1)$$

$$E(z) = g_1(z).E_c + [1 - g_1(z)].E_m \text{ for } 0 \le z \le h/2$$

$$E(z) = g_2(z).E_c + [1 - g_2(z)].E_m \text{ for } -h/2 \le z \le 0$$

where p is the volume fraction exponent, and the properties of the ceramic and metal materials are represented by Ec and Em, respectively.

To determine the different effective characteristics of metal-ceramic plates, the power law hypothesis is used as a simple rule regarding mixtures. As shown in equation (1), the top surface (z= h/2) of the S-FGM plate is ceramic, while the bottom surface (z= -h/2) is metal-rich. This explains that the metal and ceramic volume fractions are high near the bottom and top surfaces of the plate, respectively.To simplify thestudy of the S-FGM plate, Poisson's ratio v is assumed to be constant across the thickness of this plate.

Figure 2 shows the distribution of the volume fraction across the thickness of the S-FGM plate for different values of the power law index **p**. From this figure, for p=1, the composition of the ceramic and the metal varies linearly, while the p values of zero and infinity represent an all-ceramic and all-metal plate, respectively.

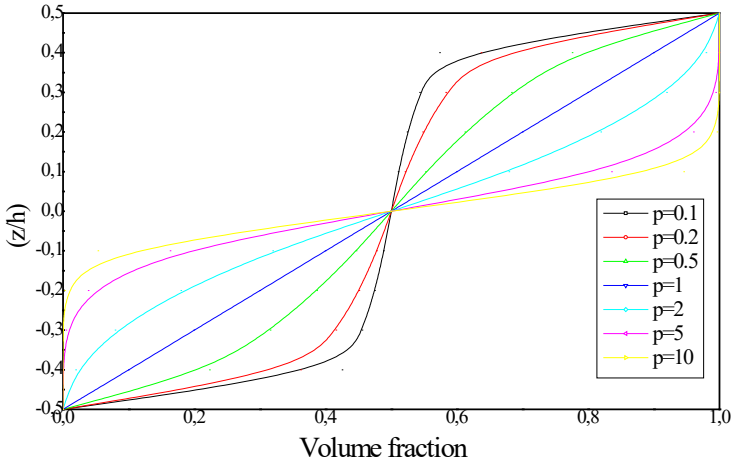

Figure 2 – Volume fraction distribution across the thickness of the S-FGM plate

Refined theory assumptions

The RPT theory is based on the following four important assumptions:

1. The strains involved are infinitesimal since the displacements are small compared to the thickness of the plate.
2. The transverse displacement W is decomposed into two components: bending w_b and shear w_s, which depend only on the x and y coordinates.

$$W(x,y,z) = w_b(x,y) + w_s(x,y) \quad (2)$$

3. The transverse normal stress σ_z is negligible compared to the other stresses σ_x and σ_y.
4. The U and V displacements in the x and y directions respectively consist of bending, shear components, and extension.

$$u = u_0 + u_b + u_s, \qquad v = v_0 + v_b + v_s \quad (3)$$

The bending components u_b and v_b are assumed to be similar to the displacements described by the classical plate theory (CPT). Therefore,

the expressions for these components can be formulated as follows:

$$u_b = -z\frac{\partial w_b}{\partial x}, v_b = -z\frac{\partial w_b}{\partial y} \qquad (4a)$$

The strain components γ_{xz} and $\gamma_{yz}$are derived component displacement state u(x,y,z) and v(x,y,z) respectively, together with the transverse displacement w(x,y,z), as shown in equation 5.These strains vary parabolically across the thickness of the S-FGM plate, while satisfying the condition of zero shear stress τ_{xz} and τ_{yz} at the top and bottom surfaces of this plate. Therefore, the expressions for u_s and $v_s$can be formulated as:

$u_{s=}f(z)\frac{\partial w_s}{\partial x}$,$v_{s=}f(z)\frac{\partial w_s}{\partial y}$(4.b)

Constitutive equations and kinematics

The displacement field of the S-FGM plate can be found by exploiting the assumptions of the refined theory and using the following equations:

$$\begin{gathered} u(x,y,z) = u_0(x,y) - z\frac{\partial w_b(x,y)}{\partial x} - f(z)\frac{\partial w_s(x,y)}{\partial x} \\ v(x,y,z) = v_0(x,y) - z\frac{\partial w_b(x,y)}{\partial y} - f(z)\frac{\partial w_s(x,y)}{\partial y} \qquad (5) \\ w(x,y,z) = w_b(x,y) + w_s(x,y) \\ f(z) = z - \left(\frac{h}{\pi}\right) * sin(\pi * z/h) \end{gathered}$$

where f(z) is Touratier's shear function. The deformations associated with the displacements in equation 5 are:

$$\begin{Bmatrix} \varepsilon_x \\ \varepsilon_y \\ \gamma_{xy} \end{Bmatrix} = \begin{Bmatrix} \varepsilon_x^0 \\ \varepsilon_y^0 \\ \gamma_{xy}^0 \end{Bmatrix} + z\begin{Bmatrix} k_x^b \\ k_y^b \\ k_{xy}^b \end{Bmatrix} + f(z)\begin{Bmatrix} k_x^s \\ k_y^s \\ k_{xy}^s \end{Bmatrix}; \begin{Bmatrix} \gamma_{yz} \\ \gamma_{xz} \end{Bmatrix} = g(z)\begin{Bmatrix} \gamma_{yz}^0 \\ \gamma_{xz}^0 \end{Bmatrix}; \varepsilon_z = 0 \quad (6)$$

where $\begin{Bmatrix} \varepsilon_x^0 \\ \varepsilon_y^0 \\ \gamma_{xy}^0 \end{Bmatrix} = \begin{Bmatrix} \frac{\partial u_0}{\partial x} \\ \frac{\partial v_0}{\partial x} \\ \frac{\partial u_0}{\partial y} + \frac{\partial v_0}{\partial x} \end{Bmatrix}, \begin{Bmatrix} k_x^b \\ k_y^b \\ k_{xy}^b \end{Bmatrix} = \begin{Bmatrix} -\frac{\partial^2 w_b}{\partial x^2} \\ -\frac{\partial^2 w_b}{\partial y^2} \\ -2\frac{\partial^2 w_b}{\partial x \partial y} \end{Bmatrix}, \begin{Bmatrix} k_x^s \\ k_y^s \\ k_{xy}^s \end{Bmatrix} = \begin{Bmatrix} -\frac{\partial^2 w_s}{\partial x^2} \\ -\frac{\partial^2 w_s}{\partial y^2} \\ -2\frac{\partial^2 w_s}{\partial x \partial y} \end{Bmatrix}$ and

$$\begin{Bmatrix} \gamma_{yz}^{0} \\ \gamma_{xz}^{0} \end{Bmatrix} = \begin{Bmatrix} \frac{\partial w_s}{\partial y} \\ \frac{\partial w_s}{\partial x} \end{Bmatrix} \quad (7)$$

$$g(z) = 1 - f^{'}(z)$$

The stress-strain relationships of an S-FGM plate can be expressed as:

$$\begin{Bmatrix} \sigma_x \\ \sigma_y \\ \tau_{xy} \\ \tau_{yz} \\ \tau_{xz} \end{Bmatrix} = \begin{bmatrix} Q_{11} & Q_{12} & 0 & 0 & 0 \\ Q_{12} & Q_{22} & 0 & 0 & 0 \\ 0 & 0 & Q_{66} & 0 & 0 \\ 0 & 0 & 0 & Q_{44} & 0 \\ 0 & 0 & 0 & 0 & Q_{55} \end{bmatrix} \begin{Bmatrix} \varepsilon_x \\ \varepsilon_y \\ \gamma_{xy} \\ \gamma_{yz} \\ \gamma_{xz} \end{Bmatrix} \quad (8)$$

where ε_x , ε_y, γ_{xy}, γ_{yz}, γ_{xz} are the strain components, and σ_x ,σ_y, τ_{xy}, τ_{yz}, τ_{xz} are the stress components. In accordance withdifferent properties of metal and ceramic materials specified in equation (1), the expressions of the stiffness coefficients Q_{ij} can be given as:

$$Q_{11} = Q_{22} = \frac{E(z)}{1-\nu^2}; \quad Q_{12} = \frac{\nu\, E(z)}{1-\nu^2}; Q_{44} = Q_{55} = Q_{66} = \frac{E(z)}{2(1+\nu)} \quad (9)$$

Equilibrium equations

The principle of virtual displacements can be used to derive the equilibrium equations, and in the present case, the principle of virtual

$$\int_{-h/2}^{h/2} \int_{\Omega} \left[\sigma_x \delta\, \varepsilon_x + \sigma_y \delta\, \varepsilon_y + \tau_{xy} \delta\, \gamma_{xy} + \tau_{yz} \delta\, \gamma_{yz} + \tau_{xz} \delta\, \gamma_{xz}\right] d\Omega\, dz - \int_{\Omega} q\, \delta\, w d\Omega = 0 \quad (10)$$

where Ω is the top surface of the S-FGM plate.
By substituting equations (5), (6), and (8) into equation (10) and integrating it through the plate thickness, equation (11) can be written as:

$$\int_{\Omega} (N_x \delta\varepsilon_x^0 + N_y \delta\, \varepsilon_y^0 + N_{xy} \delta\varepsilon_{xy}^0 + M_x^b \delta\, k_x^b + M_y^b \delta\, k_y^b + M_{xy}^b \delta\, k_{xy}^b + M_x^s \delta\, k_x^s + M_y^s \delta\, k_y^s + M_{xy}^s \delta\, k_{xy}^s$$
$$+ S_{yz}^s \delta\, \gamma_{yz} + S_{xz}^s \delta\, \gamma_{xz}) d\Omega - \int_{\Omega} q(\delta w_b + \delta w_s) d\Omega = 0 \quad (11)$$

$$\left(N_x\, , N_y N_{xy}\right) = \int_{-\mathrm{h}/2}^{\mathrm{h}/2} (\sigma_x, \sigma_y\, \tau_{xy})\, dz\, ; \left(M_x^b, M_y^b\, , M_{xy}^b\right) = \int_{-\mathrm{h}/2}^{\mathrm{h}/2} (\sigma_x, \sigma_y\, \tau_{xy})\, z\, dz$$

$$\left(M_x^s, M_y^s, M_{xy}^s\right) = \int_{-h/2}^{h/2} (\sigma_x, \sigma_y\, \tau_{xy}) f(z)\, dz;$$

$$\left(S_{xz}^s, S_{yz}^s\right) = \int_{-\frac{h}{2}}^{\frac{h}{2}} (\tau_{xz}, \tau_{yz}) g(z) dz \quad (12)$$

By substituting equation (8) into equation (12) and then integrating equation (12) through the thickness of the plate, equation (13) can be written as follows:

$$\begin{Bmatrix} N_x \\ N_y \\ M_x^b \\ M_y^b \\ M_x^s \\ M_y^s \end{Bmatrix} = \begin{bmatrix} A_{11} & A_{12} & B_{11}\, B_{12} & B_{11}^s & B_{12}^s \\ A_{12} & A_{22} & B_{12}\, B_{22} & B_{12}^s & B_{22}^s \\ B_{11} & B_{12} & D_{11}\, D_{12} & D_{11}^s & D_{12}^s \\ B_{12} & B_{22} & D_{12}\, D_{22} & D_{12}^s & D_{22}^s \\ B_{11}^s & B_{12}^s & D_{11}^s\, D_{12}^s & H_{11}^s & H_{12}^s \\ B_{12}^s & B_{22}^s & D_{12}^s\, D_{22}^s & H_{12}^s & H_{22}^s \end{bmatrix} \begin{Bmatrix} \varepsilon_x^0 \\ \varepsilon_y^0 \\ k_x^b \\ k_y^b \\ k_x^s \\ k_y^s \end{Bmatrix};$$

$$\begin{Bmatrix} N_{xy} \\ M_{xy}^b \\ M_{xy}^s \end{Bmatrix} = \begin{bmatrix} A_{66} & B_{66} & B_{66}^s \\ B_{66} & D_{66} & D_{66}^S \\ B_{66}^s & D_{66}^S & H_{66}^s \end{bmatrix} \begin{Bmatrix} \gamma_{xy}^0 \\ k_{xy}^b \\ k_{xy}^s \end{Bmatrix}; \begin{Bmatrix} S_{yz}^s \\ S_{xz}^s \end{Bmatrix} = \begin{bmatrix} A_{44}^s & 0 \\ 0 & A_{55}^s \end{bmatrix} \begin{Bmatrix} \gamma_{yz} \\ \gamma_{zx} \end{Bmatrix} \quad (13)$$

$$\left(A_{ij}, B_{ij}, D_{ij}, B_{ij}^s, D_{ij}^s, H_{ij}^s\right) = \int_{-h/2}^{h/2} (1, z, z^2, f(z), zf(z), f^2(z)) Q_{ij} dz \quad (14)$$

And $A_{ij}^s = \int_{-h/2}^{h/2} g(z)^2 * Q_{ij} dz$

By integrating equation (11) by parts, and setting the coefficients $\delta u_0; \delta v_0; \delta w_b$ and δw_s to zero separately, the resulting equilibrium equations for this FGM plate are:

$$\begin{aligned} \delta u_0 &: \frac{\partial N_x}{\partial x} + \frac{\partial N_{xy}}{\partial y} = 0 \\ \delta v_0 &: \frac{\partial N_{xy}}{\partial x} + \frac{\partial N_y}{\partial y} = 0 \\ \delta w_b &: \frac{\partial^2 M_x^b}{\partial x^2} + 2\frac{\partial^2 M_{xy}^b}{\partial x \partial y} + \frac{\partial^2 M_y^b}{\partial y^2} + q = 0 \\ \delta w_s &: \frac{\partial^2 M_x^s}{\partial x^2} + 2\frac{\partial^2 M_{xy}^s}{\partial x \partial y} + \frac{\partial^2 M_y^s}{\partial y^2} + \frac{\partial S_{xz}^s}{\partial x} + \frac{\partial S_{yz}^s}{\partial y} + q = 0 \end{aligned} \quad (15)$$

Analytical solutions for S-FGM plates

Navier presented the external force in the form of a double trigonometric series in order to solve this problem:

$$q(x,y) = \sum_{m=1}^{\infty}\sum_{n=1}^{\infty} q_{mn} sin\left(\frac{m\pi}{a}x\right) sin\left(\frac{n\pi}{b}y\right) \quad (16)$$

In the case of application of a distributed sinusoidal load, m and q_{11} are the following:

m=n=1 and $q_{11} = q_0$; $\lambda = \frac{m\pi}{a}$; $\mu = \frac{n\pi}{b}$ (17)

where q0 is the intensity of the charge in the center of this S-FGM plate.

By satisfying the boundary conditions and from Navier's solution, the displacements u_0, v_0, w_b and w_s can be written in the form of double Fourier series.

$$\begin{Bmatrix} u_0 \\ v_0 \\ w_b \\ w_s \end{Bmatrix} = \sum_{m=1}^{\infty}\sum_{n=1}^{\infty} \begin{Bmatrix} U_{mn}\cos(\lambda x)\sin(\mu y) \\ V_{mn}\sin(\lambda x)\cos(\mu y) \\ W_{bmn}\sin(\lambda x)\sin(\mu y) \\ W_{smn}\sin(\lambda x)\sin(\mu y) \end{Bmatrix} \quad (18)$$

where U_{mn} , V_{mn}, W_{bmn} , and W_{smn} are considered as arbitrary parameters to be determined.

After substitution and simplification, the following operator equation is obtained:

$$[K]\{\Delta\}^T = \{F\} \quad (19)$$

$\{\Delta\} = \{U_{mn}, V_{mn}, W_{bmn}, W_{smn}\}$; $[K]$ is the symmetric matrix given by:

$$[K] = \begin{bmatrix} a_{11} & a_{12} & a_{13} & a_{14} \\ a_{12} & a_{22} & a_{23} & a_{24} \\ a_{13} & a_{23} & a_{33} & a_{34} \\ a_{14} & a_{24} & a_{34} & a_{44} \end{bmatrix} \quad \text{And} \quad \{F^T\} = \{0,0,-q_{mn},-q_{mn}\} \quad (20)$$

for which

$$a_{11} = -\left(A_{11}\lambda^2 + A_{66}\mu^2\right)$$

$$a_{12} = -\lambda\,\mu\left(A_{12} + A_{66}\right)$$

$$a_{13} = +\lambda\left[B_{11}\lambda^2 + \left(B_{12} + 2B_{66}\right)\mu^2\right]$$

$$a_{14} = \lambda\left[B_{11}^{s}\lambda^{2} + (B_{12}^{s} + 2B_{66}^{s})\,\mu^{2}\right]$$

$$a_{22} = -A_{66}\lambda^{2} - A_{22}\mu^{2}$$

$$a_{23} = \mu\left[(B_{12} + 2B_{66})\lambda^{2} + B_{22}\mu^{2}\right]$$

$$a_{24} = \mu\left[(B^{s}{}_{12} + 2B^{s}{}_{66})\lambda^{2} + B^{s}{}_{22}\mu^{2}\right] \qquad (21)$$

$$a_{33} = -D_{11}\lambda^{4} - 2(D_{12} + 2D_{66})\lambda^{2}\mu^{2} + D_{22}\mu^{4}$$

$$a_{34} = -D_{11}^{s}\lambda^{4} - 2(D_{12}^{s} + 2D_{66}^{s})\lambda^{2}\mu^{2} - D_{22}^{s}\mu^{4}$$

$$a_{44} = -H_{11}^{s}\lambda^{4} - 2(H_{11}^{s} + 2H_{66}^{s})\lambda^{2}\mu^{2} - H_{22}^{s}\mu^{4} - A_{55}^{s}\lambda^{2} - A_{44}^{s}\mu^{2}$$

Numerical results and discussions

The results were obtained for S-FGM plates and compared withthose determined by the classical plate theory (CPT) and the high-order shear deformation theory (HSDT) (Reddy, 1984) to validate the presented theory.

$f(z) = z - \frac{h}{\pi}\sin\left(\frac{z}{h}\right)$[Touratier 1991](22.a)

$f(z) = z - z\left(1 - \frac{4z^{2}}{3h^{2}}\right)$[Reddy1984](22.b)

To carry out this analytical study on the S-FGM plate by applying the presented method, aluminum (Al) and alumina (Al_2O_3) were used as metal and ceramic, respectively, for this plate. These materials possess the following properties: aluminum metal ($E_m = 70GPa$, $\nu = 0.3$) and alumina ceramic ($E_c = 380GPa, \nu = 0.3$). In addition, the following different dimensionless parameters were used:

$$\bar{w} = \frac{10h^{3}E_{c}}{q_{0}a^{4}}w\left(\frac{a}{2},\frac{b}{2}\right),\ \overline{\sigma_{x}} = \frac{h}{q_{0}a}\sigma_{x}\left(\frac{a}{2},\frac{b}{2},\frac{h}{2}\right),\ \bar{\sigma}_{y} = \frac{h}{q_{0}a}\sigma_{y}\left(\frac{a}{2},\frac{b}{2},\frac{h}{3}\right),$$

$$\bar{\tau}_{xy} = \frac{h}{q_{0}a}\tau_{xy}\left(0,0,-\frac{h}{3}\right),\quad \bar{\tau}_{yz} = \frac{h}{q_{0}a}\tau_{yz}\left(\frac{a}{2},0,\frac{h}{6}\right),\quad \bar{\tau}_{xz} = \frac{h}{q_{0}a}\tau_{xz}\left(0,\frac{b}{2},0\right),$$

Table 1 – Dimensionless deflections and stresses for a square S-FGM plate, subjected to a sinusoidal load (a/h=10), obtained by the presented theory and the HSDT

P	$\bar{w}$		$\bar{\sigma}_x$		$\bar{\sigma}_y$		$\bar{\tau}_{yz}$	
	HSDT	Present	HSDT	Present	HSDT	Present	HSDT	Present
Ceramic	0.2960	0.2960	1.9943	1.9955	1.3124	1.3121	0.2121	0.2132
1	0.5890	0.5889	3.0850	3.0870	1.4898	1.4894	0.2608	0.2622
2	0.6551	0.6550	3.1915	3.1935	1.5992	1.5988	0.2916	0.2930
3	0.6912	0.6911	3.2663	3.2682	1.6398	1.6395	0.3117	0.3129
4	0.7120	0.7119	3.3126	3.3145	1.6540	1.6537	0.3249	0.3261
5	0.7248	0.7247	3.3421	3.3440	1.6589	1.6586	0.3336	0.3347
6	0.7332	0.7331	3.3617	3.3636	1.6606	1.6603	0.3394	0.3404
7	0.7390	0.7388	3.3754	3.3773	1.6613	1.6610	0.3432	0.3442
8	0.7431	0.7430	3.3852	3.3871	1.6616	1.6613	0.3457	0.3466
9	0.7462	0.7460	3.3925	3.3944	1.6618	1.6615	0.3473	0.3483
10	0.7485	0.7483	3.3980	3.3999	1.6619	1.6616	0.3484	0.3493
Metal	1.6071	1.6070	1.9943	1.9955	1.3124	1.3121	0.2121	0.2132

P	$\bar{\tau}_{xz}$		$\bar{\tau}_{xy}$	
	HSDT	Present	HSDT	Present
Ceramic	0.2386	0.2462	0.7067	0.7065
1	0.2386	0.2462	0.6111	0.6110
2	0.2373	0.2447	0.5212	0.5211
3	0.2361	0.2434	0.4902	0.4902
4	0.2354	0.2425	0.4857	0.4856
5	0.2348	0.2418	0.4893	0.4892
6	0.2345	0.2414	0.4943	0.4942
7	0.2342	0.2411	0.4987	0.4986
8	0.2340	0.2408	0.5022	0.5021
9	0.2338	0.2407	0.5050	0.5048
10	0.2337	0.2405	0.5071	0.5070
Metal	0.2386	0.2462	0.7067	0.7065

Table 1 illustrates different dimensionless deflections and stresses of a square S-FGM plate, subjected to a sinusoidal load with a ratio a/h=10, for different values of the power law index **p**, obtained by the present refined plate theory (RPT) and the HSDT. As shown in this table, and since both theories take into account the transverse shear effect, the results obtained by the present theory, both for deflection and stresses, are in agreement with those obtained by Reddy's high-order shear deformation

theory. In addition, the dimensionless deflection $\overline{w}$ and the longitudinal stresses $\overline{\sigma}_x$,$\overline{\sigma}_y$ in the plane are directly proportional to the increase in the power law index **p**. It should also be noted that the stresses for the ceramic plate are identical to those for the metal plate, since this S-FGM plate in both cases is completely homogeneous and these stresses are independent of the modulus of elasticity.

Table 2 – Dimensionless deflections and transverse shear stresses of the square S-FGM plate calculated by the present theory, HSDTand CPT

a/h	***p***	$(wE_c)/(q_0h)$			$\tau_{xz}(0, b/2)/q_0$	
		CPT	HSDT	Present	HSDT	Present
	0.25	0.3049	0.3715	0.3714	0.1191	0.1228
	0.5	0.3207	0.3874	0.3873	0.1192	0.1230
5	1	0.3514	0.4180	0.4178	0.1190	0.1228
	4	0.4288	0.4936	0.4932	0.1175	0.1209
	10	0.4518	0.5157	0.5152	0.2387	0.2463
	0.25	4.8782	5.1453	5.1450	0.2386	0.2462
	0.5	5.1310	5.3985	5.3981	0.2389	0.2465
10	1	5.6228	5.8895	5.8891	0.2386	0.2462
	4	6.8604	7.1200	7.1187	0.2354	0.2425
	10	7.2289	7.4849	7.4831	0.2337	0.2405

Table 2 shows a comparative study of the deflections and transverse shear stresses of a simply supported square S-FGM functionally graded plate, subjected to a sinusoidal load with two ratios (a/h=5 and a/h=10) for five values of the power law exponent **p**, calculated by the present, HSDT and CPT theories. According to these results, it can be confirmed that there is an excellent agreement between the values of deflection and transverse shear stress obtained by the present theory and HSDTs, for all values of the power law exponent **p** and the two ratios a/h. On the other hand, the classical platetheory (CPT) underestimates transverse plate displacement because it does not take into account the impacts of transverse shear deformation, which is the biggest disadvantage of this theory.

The analytical values illustrated in Tables 1 and 2 demonstrate the effectiveness of this present theory in the study of S-FGM plates because its results are in high agreement with theHSDTand better than the CPT.

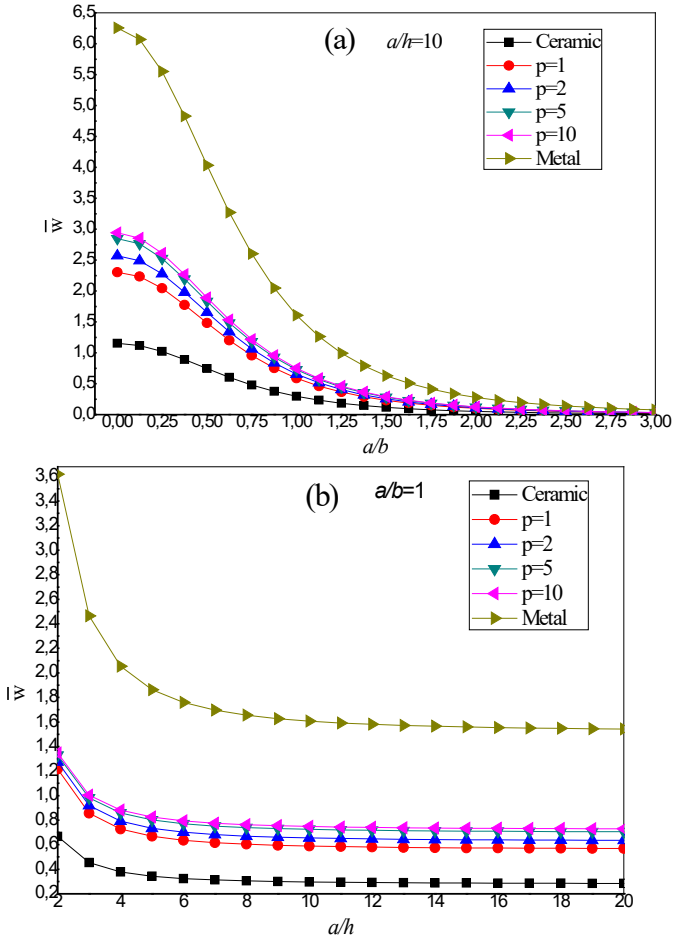

Figure 3 – $\overline{w}$ vs ratios: (a) - a/b, (b) - a/h, of an S-FGM plate

Figures 3-a and 3-b show the evolution of the dimensionless deflection $\overline{w}$ as a function of the thickness ratios a/b and a/h of an S-FGM plate, respectively, for different values of the power law index **p**using the present theory. The present theory shows that the dimensionless deflection of the S-FGM plate decreases sharply within the ranges of 0 to 1.5 and 2 to 8 for the ratios a/b and a/h, respectively; after that, it becomes less affected by these ratios.

According to these results, the deflection values of the metal plate are higher than those of the ceramic plate. They increase with the power law index **p** and remain almost constant when going from a moderately thick to a very thick plate. This indicates that the response of the S-FGM

plate lies between those of isotropic plates, i.e., between the ceramic-rich plate and the metal-rich plate.

In this section of our analytical study, the distribution of different shear stresses of the S-FGM plate under a sinusoidal load was investigated, where the exponent of the volume fraction of this plate is p=2.

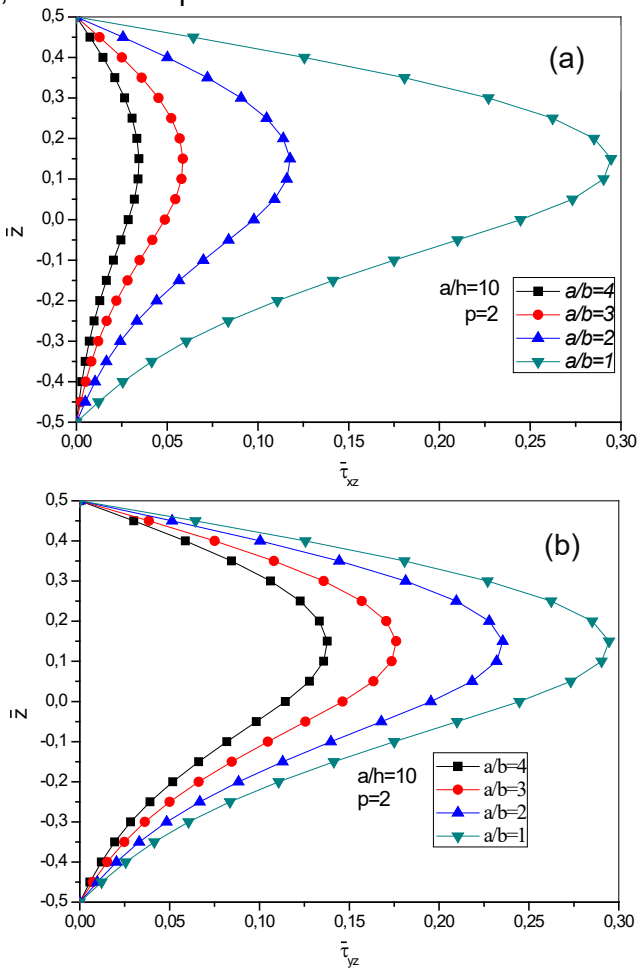

Figure 4 – Distribution of stresses: (a) - $\bar{\tau}_{xz}$, (b) - $\bar{\tau}_{yz}$, across the thickness of the S-FGM plate

Figures 4-a and 4-b respectively represent the variation of the transverse tangential stresses $\bar{\tau}_{xz}$ and $\bar{\tau}_{yz}$ across the thickness of an S-FGM plate for different a/b ratios. These shear stress values are zero at the two top and bottom edges of the plate and then gradually increase with decreasing the a/b ratio, reaching the maximum values at $\bar{z} = 0.154$, which

represents the inhomogeneous case. Moreover, the maximum values of $\overline{\tau}_{yz}$ stresses are larger compared to those of $\overline{\tau}_{xz}$ at the ratios a/b=2, 3, and 4.

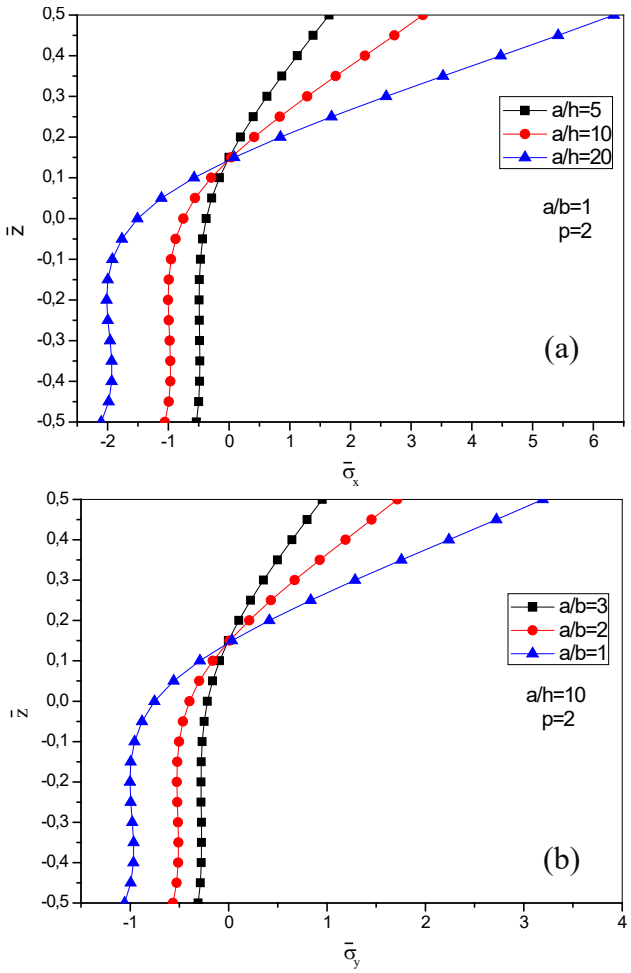

Figure 5 – Distribution of normal stresses: (a) - $\overline{\sigma}_x$, (b) - $\overline{\sigma}_y$, across the thickness of the S-FGM plate

Figures 5-a and 5-b show the variation of the normal stresses $\overline{\sigma}_x$ and $\overline{\sigma}_y$ according to the thickness of an S-FGM plate for different values of the ratios a/b and a/h, respectively. As shown in these figures, the normal stresses are in compressive throughout the S-FGM plate up to $\bar{z} = 0.154$, then in tensile beyond this value. Furthermore, the maximum compressive and tensile values of these stresses are produced respectively at points

located on the bottom surface and the top surface of this plate. In addition, for the normal stresses $\overline{\sigma}_x$, and when the a/h ratio increases, the tensile stress at the top surface increases, while the compressive stress at the bottom surface decreases for this S-FGM plate. On theother hand, and for normal stresses $\overline{\sigma}_y$, the tensile and compressive stresses decrease and increase respectively as a function of the increase in the ratio a/b, as shown in Figures 5-a and 5-b.

According to the results of the variation of the transverse tangential stress $\overline{\tau}_{xy}$ across the thickness of the S-FGM plate for the three values of a/b ratio, presented in Figure 6, the tensile and compressive stresses occur on the bottom and top surfaces of this plate, respectively, and this is inconsistent with what was found for the normal stresses $\overline{\sigma}_x$ and $\overline{\sigma}_y$. Furthermore, the zero value of this transverse tangential stress corresponds to $\bar{z} = 0.154$.

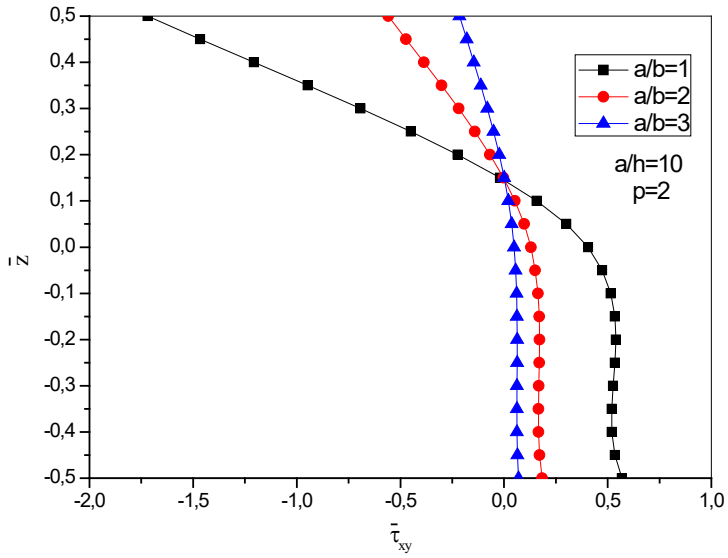

Figure 6 – Distribution of the transverse tangential stress $\overline{\tau}_{xy}$ across the thickness of the S-FGM plate

Figure 7 shows the effect of the moduli ratios Em/Ec on the dimensionless deflection $\overline{w}$ of S-FGM plates with various ceramic-metal mixtures p studied at a thickness of a/h = 10. As shown in these results, the dimensionless deflection is strongly affected by the moduli ratios, as it decreases significantly with these ratios up to the value Em/Ec = 0.25, after which this effect diminishes. In addition, the dimensionless deflection

increases with the increase in the percentage of metal (aluminum) in the plate made of a mixture of metal and ceramic.

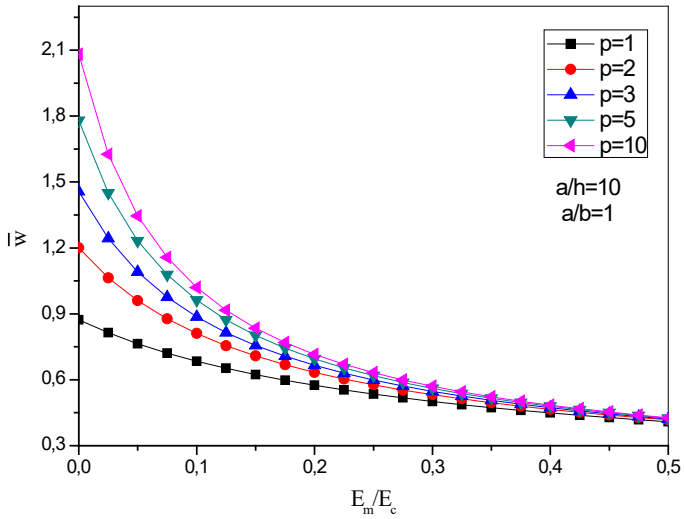

Figure 7 – $\bar{w}$ vs E_m/E_c ratio of the S-FGM plate

Conclusion

In this work, a refined two-variable theory was presented for the bending analysis of S-FGMs plates with ceramic-metal mixture and under sinusoidal load distribution. Although no shear correction factors were used, this theory satisfied the conditions of zero shear stresses on the plate surfaces and gave a parabolic distribution of transverse shear stresses. The calculated different stresses and dimensionless displacements clearly demonstrated the effectiveness and accuracy of the present theory to study the static behaviors of simply supported S-FGM plates.The comparison between the present refined theory and the HSDT (Reddy's theory) also showed that the deformations and stresses of these theories are almost identical, while the classical plate theory underestimates the deflection of these plates. It was observed from the results obtained that there is an excellent agreement between the deflections of ceramic plates and those rich in metals, while the deflection value is directly proportional to the power law index **p**, which proves the importance of gradients in material properties in determining the response of S-FGM plates.

References

Abdulrazzaq, M., A., Fenjan, R., M., Ahmed, R., A., Faleh, N., M. 2020. Thermal buckling of nonlocal clamped exponentially graded plate according to a

secant function based refined theory. *Steel Compos Struct,* 35(1),pp.147-157. Available at: https//doi.org/10.12989/scs.2020.35.1.147

Ahmed, R., A., Fenjan, R., M., Faleh, N., M. 2019. Analyzing post-buckling behavior of continuously graded FG nanobeams with geometrical imperfections. *Geomechanics and Engineering*, 17(2), pp.175-180. Available at: https//doi.org/10.12989/gae.2019.17.2.175

Avcar, M. 2015. Effects of rotary inertia shear deformation and non-homogeneity on frequencies of beam. *Struct. Eng. Mech,*55(4), pp.871-884. Available at: https//doi.org/10.12989/sem.2015.55.4.871

Beldjelili, Y., Tounsi, A., Mahmoud, S., R. 2016.Hygro-thermo-mechanical bending of S-FGM plates resting on variable elastic foundations using a four-variable trigonometric plate theory. *Smart Structures and Systems,* 18(4), pp.755-786. Available at: https//doi.org/10.12989/sss.2016.18.4.755

Birman, V., Keil, T., Hosder, S. 2013. Functionally graded materials in engineering. In: S Thomopoulus, V Birman and GM Genin (eds) Structural interfaces and attachments in biology. *New York: Springer,*pp.19–41. Available at: https//doi.org/10.1007/978-1-4614-3317-0_2

Boukhari, A., Ait Atmane, H., Houari, M., S., A., Tounsi, A., AddBedia, E., A., Mahmoud, S., R. 2016.An efficient sheadeformation theory for wave propagation of functionally gradedmaterial plates. *Struct. Eng. Mech,* 57(5), pp.837-859. Available at: https//doi.org/10.12989/sem.2016.57.5.837

Chi, S., H. Chung, Y., L. 2006. Mechanical behavior of functionally graded material plates under transverse load—Part I: Analysis. International Journal of Solids and Structures, 43(13), pp.3657-3674. Available at: https//doi.org/10.1016/j.ijsolstr.2005.04.011

Dai, H., L., Rao, Y., N., Dai, T. 2016. A review of recent researches on FGM cylindrical structures under coupled physical interactions. *Compos Struct,*152, pp.199–225. Available at: https//doi.org/10.1016/j.compstruct.2016.05.042

Dehshahri, K., Nejad, M., Z., Ziaee, S., Niknejad, A., Hadi, A. 2020. Free vibrations analysis of arbitrary threedimensionally FGM nanoplates. *Adv. Nano Res,* 8(2), pp.115-134. Available at: https//doi.org/10.12989/anr.2020.8.2.115

Duc, N., D., Quang, V., D., Anh, V., T., T. 2017. The nonlinear dynamic and vibration of the S-FGM shallow spherical shells resting on an elastic foundations including temperature effects. *Int. J. Mech. Sci,* 123,pp. 54–63. Available at: https//doi.org/10.1016/j.ijmecsci.2017.01.043

Eltaher, M., A., Alshorbagy, A., E., Mahmoud, F., F. 2013.Determination of neutral axis position and its effect on natural frequencies of functionally graded macro/nanobeams. *Composite Structures*, 99, pp.193-201. Available at: https//doi.org/10.1016/j.compstruct.2012.11.039

Fallah, A., Aghdam, M., M., Kargarnovin, M., H. 2013. Free vibration analysis of moderately thick functionally graded plates on elastic foundation using the extended Kantorovich method. *Arch. Appl. Mech,* 83(2), pp.177-191. Available at: https//doi.org/10.1007/s00419-012-0645-1

Hosseini-Hashemi, S., Rokni Damavandi Taher, H., Akhavan, H., Omidi, M. 2010. Free vibration of functionally graded rectangular plates using first-order

shear deformation plate theory. *Appl. Math. Model,* 34(5), pp.1276-1291. Available at: https//doi.org/10.1016/j.apm.2009.08.008

Hosseini-Hashemi, S., Fadaee, M., Atashipour, S., R. 2011. A new exact analytical approach for free vibration of ReissnerMindlin functionally graded rectangular plates. *Int. J. Mech.Sci,*53(1), pp.11-22. Available at: https//doi.org/10.1016/j.ijmecsci.2010.10.002

Kar, V., R., Panda, S., K. 2015.Nonlinear flexural vibration of shear deformable functionally graded spherical shell panel. *Steel Compos. Struct, Int. J.*, 18(3), pp.693-709. Available at: https//doi.org/10.12989/scs.2015.18.3.693

Karakoti, A., Pandey, S., Kar, V., R. 2022. Nonlinear transient analysis of porous P-FGM and S-FGM sandwich plates and shell panels under blast loading and thermal environment. *Thin-Walled Structures,*173, 108985. Available at: https//doi.org/10.1016/j.tws.2022.108985

Karami, B., Karami, S. 2019. Buckling analysis of nanoplate-type temperature-dependent heterogeneous materials. *Advances in Nano Research*, 7(1), pp.51-61. Available at: https//doi.org/10.12989/anr.2019.7.1.051

Kumar, A., Pandey, S. 2024. Transient analysis of size-dependent S-FGM micro-folded plates based on exact shear correction factor in the thermal environment. *Arch Appl Mech*, 94, pp.1335–1357. Available at: https//doi.org/10.1007/s00419-024-02578-6

Kurpa, L., Shmatko, T., Awrejcewicz, J., Timchenko, G., Morachkovska, I. 2023, Analysis of Free Vibration of Porous Power-law and Sigmoid Functionally Graded Sandwich Plates by the R-functions Method. *Journal of Applied and Computational Mechanics,*9(4), pp.1144-1155. Available at: https//doi.org/10.22055/jacm.2023.43435.4082

Mechab, I., Ait Atmane, H., Tounsi, A., Belhadj, H., A., Adda Bedia, El-A. 2010. A two variable refined plate theory for the bending analysis of functionally graded plates. *Acta Mech Sin*, 26, pp.941–949. Available at: https//doi.org/10.1007/s10409-010-0372-1

Pandey, H., K., Agrawal, H., Panda, S., K., Hirwani, C., K., Katariya, P., V., Dewangan, H., C. 2020. Experimental and numerical bending deflection of cenosphere filled hybrid (Glass/Cenosphere/Epoxy) composite. *Struct. Eng.Mech,*73(6),pp.715-724. Available at: https//doi.org/10.12989/sem.2020.73.6.715

Reddy, J., N.2000. Analysis of functionally graded plates. *Int. J. Numer. Method. Eng*, 47(1-3), pp.663-684. Available at: https//doi.org/10.1002/(SICI)1097-0207(20000110/30)47:1/3<663::AID-NME787>3.0.CO;2-8

Reddy, J., N. 1984. A simple higher-order theory for laminated composite plates. *J Appl Mech,*51, pp.745–52. Available at: https//doi.org/10.1115/1.3167719

Selmi, A.2020. Dynamic behavior of axially functionally graded simply supported beams. *Smart Struct. Syst,* 25(6), pp.669-678. Available at: https//doi.org/10.12989/sss.2020.25.6.669

Singh, S., J., Harsha, S., P.2019. Nonlinear dynamic analysis of sandwich S-FGM plate resting on pasternak foundation under thermal environment. *European*

*Journal of Mechanics - A/Solids,*76, pp.155-179. Available at: https//doi.org/10.1016/j.euromechsol.2019.04.005

Singh, S., J., Harsha, S., P.2020.Thermo-mechanical analysis of porous sandwich S-FGM plate for different boundary conditions using Galerkin Vlasov's method: A semi-analytical approach. *Thin-Walled Structures,* 150, 106668. Available at: https//doi.org/10.1016/j.tws.2020.106668

Sobhy, M. 2013. Buckling and free vibration of exponentially graded sandwich plates resting on elastic foundations under various boundary conditions. *Compos. Struct,* 99, pp.76-87. Available at: https//doi.org/10.1016/j.compstruct.2012.11.018

Taczała, M., Buczkowski, R., Kleiber, M. 2022. Analysis of FGM plates based on physical neutral surface using general third-order plate theory. *Composite Structures,*301, 116218. Available at: https//doi.org/10.1016/j.compstruct.2022.116218

Tao, C., Dai, T. 2021. Analyses of thermal buckling and secondary instability of post-buckled S-FGM plates with porosities based on a meshfree method. *Applied Mathematical Modelling,* 89, pp.268-284. Available at: https//doi.org/10.1016/j.apm.2020.07.032

Thai, H., T., Choi, D., H.2012.A refined shear deformation theory for free vibration of functionally graded plates on elastic foundation. *Compos. Part B: Eng,* 43(5), pp.2335-2347. Available at: https//doi.org/10.1016/j.compositesb.2011.11.062

Thai, H., T., Kim, S., E. 2013. A simple quasi-3D sinusoidal shear deformation theory for functionally graded plates. *Compos. Struct,* 99, pp.172-180. Available at: https//doi.org/10.1016/j.compstruct.2012.11.030

Touratier, M. 1991. An efficient standard plate theory. *Int J Eng Sci.* 29(8): 901–16. Available at: https//doi.org/10.1016/0020-7225(91)90165-Y

Теорија смицајне деформације вишег реда са четири непознате за анализу савијања S-FGM плоча

Фатима Зохра Џидар, *Хабиб* Хебали, **аутор за преписку**
Универзитет „Мустафа Стамболи”, Одсек за грађевинарство, Маскара, Народна Демократска Република Алжир

ОБЛАСТ:грађевинарство
КАТЕГОРИЈА (ТИП) ЧЛАНКА:оригинални научни рад

Сажетак:

Увод/циљ: Плоче од сигмоидно функционално градијентно распоређених материјала (S-FGM) испитане су на савијање помоћу теорије смицајне деформације вишег реда са четири променљиве.
Представљена теорија једноставно смањује број непознатих функција са пет на четири у односу на друге теорије које се баве смицајном деформацијом. Такође, не захтева факторе корекције

смицања и задовољава услов да не постоје смицајни напони на горњој и доњој површини плоче, будући да смицање варира у облику параболе кроз дебљину плоче. Једначине равнотеже ове теорије изведене су из принципа виртуелног рада и решавају се помоћу Навијеовог решења. На основу закона снаге, материјали ове S-FGM плоче распоређени су по запреминским уделима конституената, а њихова својства се постепено мењају по дубини. Ова аналитичка студија дала је веома задовољавајуће резултате, а поређење њених нумеричких резултата и оних добијених помоћу класичне теорије плоча (CPT) и теорија смицајне деформације вишег реда (HSDTs) указало је на једноставност, тачност и поузданост ове теорије у анализи понашања дебелих S-FGM плоча при статичком савијању.

Методе: Представљена је теорија смицајне деформације са четири променљиве којом се одређују напони и померања у једноставно ослоњеној плочи од функционално градијентно распоређених материјала (S-FGM). Једначине равнотеже и граничних услова добијене су из принципа виртуелног рада. Навијеов метод је затим примењен у решавању једначина равнотеже. Резултати ове нове теорије поређени су са решењима других теорија (CPT, HSDT).

Резултати: Поређење ове прерађене теорије и Редијеве теорије (HSDT) такође је показало да су деформације и напони ових теорија готово идентични, док класична теорија плоча потцењује дефлексију оваквих плоча.

Закључак: Израчунати различити напони и бездимензионална померања јасно показују ефикасност и тачност представљене теорије при проучавању статичких понашања једноставно ослоњених S-FGM плоча.

Кључне речи: S-FGM плоче, класична теорија плоча, теорија вишег реда, закон снаге, савијање

Paperreceivedon: 29.03.2025.
Manuscriptcorrectionssubmittedon:29.04.2025.
Paperacceptedfor publishingon: 28.05